Biomech Model Mechanobiol (2012) 11:1187–1204
DOI 10.1007/s10237-012-0414-7

ORIGINAL PAPER

Biomechanics of early cardiac development

Sevan Goenezen · Monique Y. Rennie · Sandra Rugonyi

Received: 21 February 2012 / Accepted: 20 June 2012 / Published online: 4 July 2012
© Springer-Verlag 2012

Abstract Biomechanics affect early cardiac development, from looping to the development of chambers and valves. Hemodynamic forces are essential for proper cardiac development, and their disruption leads to congenital heart defects. A wealth of information already exists on early cardiac adaptations to hemodynamic loading, and new technologies, including high-resolution imaging modalities and computational modeling, are enabling a more thorough understanding of relationships between hemodynamics and cardiac development. Imaging and modeling approaches, used in combination with biological data on cell behavior and adaptation, are paving the road for new discoveries on links between biomechanics and biology and their effect on cardiac development and fetal programming.

Keywords Early cardiac development · Cardiogenesis · Computational modeling · Computational biomechanics · Valveless pumping · Blood flow modeling

Sevan Goenezen and Monique Y. Rennie contributed equally to this manuscript.

S. Goenezen · S. Rugonyi (✉)
Department of Biomedical Engineering,
Oregon Health & Science University, Portland, OR 97239, USA
e-mail: rugonyis@ohsu.edu

S. Goenezen
e-mail: sevangoenezen@gmail.com

M. Y. Rennie
Heart Research Center, Oregon Health & Science University, Portland, OR 97239, USA
e-mail: rennie@ohsu.edu

1 Introduction

Function of the heart is essential for embryo survival, and thus the heart starts beating and pumping blood early in embryogenesis when it is still a linear tube with no valves or chambers. As such, key morphogenetic changes that transform the heart from a straight tube into a complex, multichambered structure all occur under blood flow conditions. Constant interactions between cardiac tissue motion and blood flow dynamics shape the development of the heart. In the absence of blood flow, the heart does not develop properly (Hove et al. 2003; Abu-Daya et al. 2009), and deviations from normal hemodynamic conditions lead to cardiac malformations (Sedmera et al. 1999, 2002; Tobita and Keller 2000; Clark et al. 1984; Rychter 1978). During early, tubular stages of cardiac development, the heart is very sensitive to biomechanical cues. This is despite rapid increases in blood flow and blood pressure to support the growing demands of the embryo (Keller et al. 1991; Hu and Keller 1995) and rapid structural changes which alter the patterns of flow (Yalcin et al. 2011). Although the basic plan for cardiac development is laid out within an organism's genetic blueprint (Srivastava 2006), hemodynamics modify this blueprint and thus play a large and critical role in shaping development of the heart.

Several animal models have been used to study cardiac development. Mouse models are very commonly used, most notably to study genes important for cardiac development and linked to cardiac defects (Bruneau 2008), and provide valuable information about the role of genetic perturbations. Hemodynamic conditions during early murine heart development are measurable (Zhou et al. 2002). Indeed, hemodynamic perturbations have been observed prior to midgestation lethality in transgenically altered mice (Phoon et al. 2004). However, accessing embryos within their mothers womb is difficult. To avoid these difficulties, non-mamma-

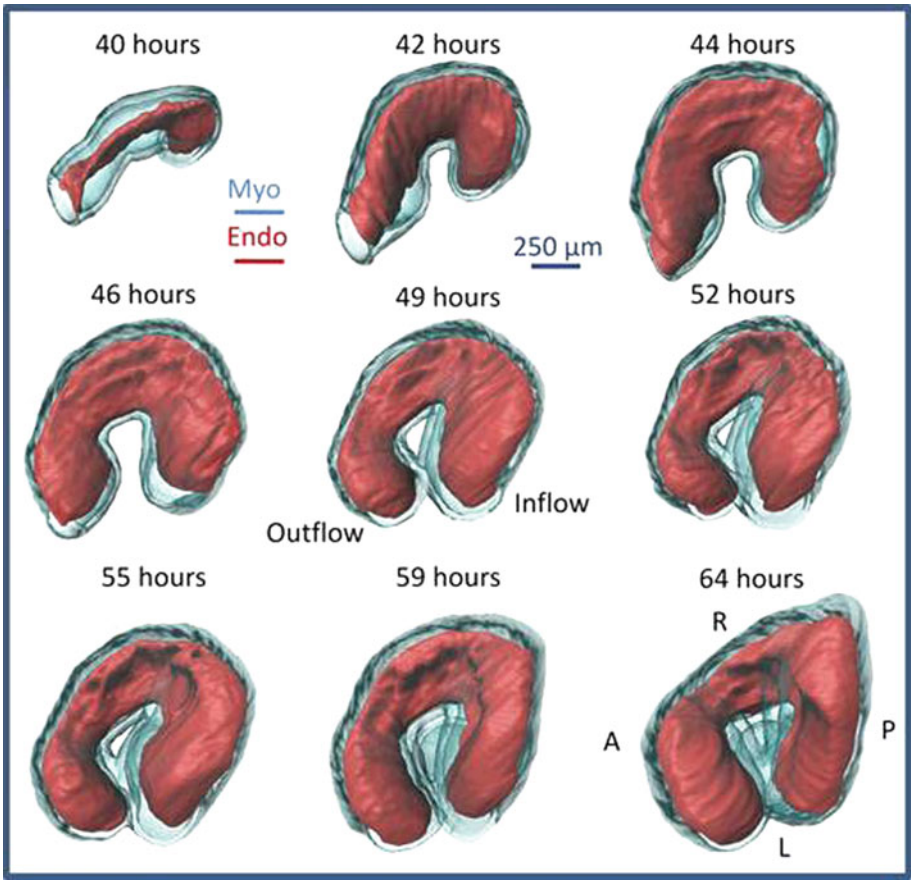

Fig. 1 3D image reconstructions from optical coherence tomography data are shown from Hamburger–Hamilton stages HH11 (40 h) up to HH18 (64 h). *Transparent blue* is the myocardium and *red* is the endocardium. *Myo* myocardium, *Endo* endocardium, *CJ* cardiac jelly, *A* anterior, *P* posterior, *D* dorsal, *V* ventral, *R* right, *L* left. Image reproduced with permission from Jenkins et al. (2012)

lian models of cardiac development have been widely used, including zebrafish, frog, and avian embryos (Miura and Yelon 2011; Warkman and Krieg 2007; Martinsen 2005). Developmental processes are highly conserved among vertebrate species; thus, these non-mammals are excellent models to study cardiac development, enabling easy access to the embryo for manipulation and imaging. Non-mammalian models have therefore been widely used to study the effects of hemodynamic conditions on heart development, for example, (Hove et al. 2003; Sedmera et al. 1999). Much has been learned about the adaptations of the heart to altered hemodynamic conditions, including detrimental adaptations that lead to congenital cardiac defects. There is still, however, much to be learned: The mechanobiological mechanisms that drive adaptations in response to hemodynamic forces are only beginning to emerge (Hogers et al. 1999; Groenendijk et al. 2007; Hierck et al. 2008; Poelmann et al. 2008; Van der Heiden et al. 2006; Egorova et al. 2011), and a full understanding of these adaptations requires quantification of biological processes as well as biomechanical factors.

Computational models of cardiac mechanics enable quantification of biomechanical cues that modulate intrinsic genetic programs. Such models are becoming ever more important in understanding embryonic, non-genetic origins of congenital heart disease. Initial computational studies have simplified cardiac geometries to provide an understanding of biomechanical factors affecting cardiac processes such as looping, and blood flow conditions in bended tubes, for example, (Loots et al. 2003). Recent advances in imaging techniques (e.g., see Fig. 1) and computational technologies are now enabling development of dynamic, subject-specific computational models of the heart, for example, (Butcher et al. 2007; Liu et al. 2011). These computational models, used in combination with biological data on cell adaptation, have the potential to revolutionize the field of cardiac development and our understanding of congenital heart disease.

This manuscript intends to summarize our current understanding of the biomechanics of cardiac morphogenesis during early stages of embryonic development, focusing on the effects of hemodynamic conditions. The early stages of heart development and the mechanics of pumping in the tubular heart are described, followed by a description of the normal physiological changes that occur during cardiac development and physiological changes which occur when hemodynamic conditions are mechanically altered. Lastly,

Table 1 Early stages of heart development in the embryonic human, chick, and mouse

	Human (days)	Chick	Mouse	Milestones
Linear heart tube	22	HH10–HH11	E8	Formation of heart tube; 1st heart beat; initiation of hemodynamic forces
Looping heart	28	HH10–HH24	E9	Heart tube increases in length; dextral looping; early formation of chambers
Trabeculation	26–32	HH17–HH25	E10	Replacement of cardiac jelly with trabeculae; stage ends with compaction
Cushion formation	28–37	HH12–HH34	E9–E11	Serve as primitive valves
Septation initiation	50–60	HH21–HH26	E11–E13	Four-chambered heart
Valve formation	42–70	HH24–HH36	E12–E17	Cushions fuse and condense to form valve leaflets

References: Martinsen (2005), Bruneau (2008), Rauhut-Klaban et al. (2008), Sedmera et al. (1997), Oostra et al. (2007), Maron and Hutchins (1974), Lincoln et al. (2004)

prior work and current efforts toward computational modeling of cardiac development are discussed and conclusions given.

2 Early cardiac development

During early cardiac development, a primitive tubular heart forms when two separate masses of precardiac mesoderm migrate to the ventral midline and meet to form a hollow tube structure. The process by which this migration occurs is not well understood; however, several lines of evidence suggest that asymmetric contraction of actin microfilaments lead to cylindrical bending of epithelial cells and the formation of a hollow tube (Taber 1998; Ettensohn 1985; Bartman and Hove 2005). The heart then transforms from a simple linear tubular structure to a four-chambered heart. This process of heart formation is remarkably similar in humans and animal models, but the staging systems used and the timing of events differ, as outlined in Table 1. In humans, developmental stages are usually referenced based on the Carnegie stages (O'Rahilly and Muller 1987, 2010), or days post-conception. In mice, an E is typically used to reference embryonic days. In chicken embryos, stages are denoted as days after incubation or, more precisely, following the Hamburger–Hamilton (HH) staging system (Hamburger and Hamilton 1992).

2.1 Tubular heart

The early cardiac tube is composed of three tissue layers: an inner monolayer of endocardium, a thick middle layer of cardiac jelly, and a two-cell layer of myocardium. Spontaneous action potentials propagate through the myocardium even before the myocytes become contractile (Kamino et al. 1981), initiating the eventual onset of blood flow.

2.2 Heart looping

In the next stage of cardiac morphogenesis, the straight heart tube transitions into a looped structure with a morphologically distinct primitive atrium, primitive ventricle, and primitive outflow tract (e.g., see Fig. 1). The looping process occurs soon after initial cardiac contractions begin. Some view the looping process as the bending of the heart tube into a c-like shape, known as dextral looping (sometimes referred to as dextro-looping), while others consider the further rotation or twisting into an s-like shape that continues into the septation phase as part of this process (Männer 2000; Bouman et al. 1995; Männer 2004).

During advanced stages of cardiac looping (s-shaped tube), regional wall thickenings of cardiac jelly form endocardial cushions in the atrio-ventricular canal and outflow tract region. During contraction, the lumen completely closes off by apposition of the endocardial cushions, which function as primitive valves facilitating pulsatile flow.

The biomechanics of dextral looping, which establishes the first morphological left-right asymmetry of the developing heart, are considered here. Dextral looping results from two mechanical processes: (1) bending toward the ventral surface of the heart and (2) rightward rotation of the bend, leading to a helical structure (Männer 2004). It is generally accepted that the direction of looping is mediated by asymmetric expression of several genetic and molecular markers (Mercola and Levin 2001; Baker et al. 2008), but intrinsic and extrinsic forces are also critical in the looping process. The torsional/rotational component of looping may be strongly influenced by extrinsic forces from neighboring tissues (Voronov and Taber 2002; Voronov et al. 2004). Further, it has been speculated that contact between the myocardial wall and neighboring membranes could lead to mechanotransduction of positional information as the cardiac loop elongates (Garita et al. 2011).

Many groups have presented evidence for forces intrinsic to the heart itself driving the bending component of looping. Differential growth of the heart tube may drive looping (Stalsberg 1970; Taber 1998). During dextral heart looping, there is an increase in length and also an increase in diameter toward the caudal region of the heart tube. Prior to looping, the dorsal mesocardium supports the tubular heart and restricts elongation along the dorsal

cardiac wall, which leads to a slight curve in the heart tube (Taber 1998). The dorsal mesocardium then ruptures during looping, and its remnants could shorten and force the heart to bend (Taber 1998). Alternatively, several groups have put forth evidence that actin filament polymerization plays an important role in bending of the walls and that its disruption prevents or perturbs looping (Latacha et al. 2005; Itasaki et al. 1991). It is possible that each of these mechanisms is required for looping. Or, given that even small perturbations in the normal looping process lead to a spectrum of congenital heart defects, there may be several redundant mechanisms in place for this critical stage in cardiac development (Taber et al. 1995).

2.3 Trabeculation and compaction

The process of trabeculation is initiated near the end of looping, when cardiac jelly is displaced from the ventricle's outer curvature and endocardial pouches grow toward the myocardial layer (Icardo and Fernandez-Teran 1987; Manner et al. 2009). Primary trabeculations and secondary offsets create a haphazard pattern of spongy tissue. While trabeculation is regulated by several developmental genes and metabolites (e.g., N-cadherin, retinoic acid, neuregulin, ErbB, and BMP-10 (Ong et al. 1998; Wagner and Siddiqui 2007; Gassmann et al. 1995; Lee et al. 1995; Meyer and Birchmeier 1995)), hemodynamics also modulate trabeculation. The hemodynamic stimulus for this change may be increased wall strain or stresses (Damon et al. 2009). Although the exact biomechanical stimuli are currently unknown, overt changes in trabecular patterning in cases of hemodynamic perturbation highlight the importance of hemodynamic conditions in regulating trabecular development and patterning (Sedmera et al. 1999).

Formation of trabeculae greatly increases surface area, myocardial mass, and wall stiffness (Yang et al. 1994). The increase in surface area increases passive diffusion of oxygen in the absence of coronary vessels at this early stage (Burggren and Keller 1997). As trabecular density increases with load, it is believed that the trabeculae aid in cardiac contraction (Challice and Virágh 1974). Trabeculae have further been implicated in facilitating more rapid conduction (de Jong et al. 1992), increasing myocardial blood flow, and aiding in the direction of blood out of the ventricle prior to septation (Yang et al. 1994; Taber 1991). After a period of trabecular growth (Table 1), trabecular compaction begins contributing to the formation of the ventricular septum and to the thickening of the ventricular compact layer (Rychterova 1971). Normal growth of the compact layer of ventricular myocardium depends on correct formation of the embryonic epicardium and coronary blood vessels (Smith and Bader 2007), which derive from the pro-epicardium and sinus venosus (cardiac inlet) endothelium.

2.4 Septation and valve development

Septation within the atrium and ventricle completes the transformation into a four-chambered heart. Interventricular septation and chamber formation is believed to occur via coalescence and compaction of trabeculae, formation and fusion of the endocardial cushions, and ballooning of the ventricles (Lamers and Moorman 2002; Van den Berg and Moorman 2009). It has long been speculated that hemodynamic forces play an important role in ventricular septation (Bremer 1932) and studies in which flow is experimentally perturbed leads to numerous defects in atrial and ventricular septation (Colvee and Hurle 1983; Hogers et al. 1997, 1999); thus, normal septation does not occur in the presence of aberrant flows.

Up until this point, endocardial cushions in the atrioventricular canal and outflow tract have served as primitive valves. Valvulogenesis begins with the formation of endocardial cushions in the atrioventricular (AV) canal and outflow tract. These cushions are the result of localized extracellular matrix deposition between the endocardial and myocardial layers of the heart tube, which run along the heart loop downstream of the primitive atrium (Manner et al. 2008). Remnants of displaced cardiac jelly remain as endocardial cushions (Manner et al. 2008, 2009) which are colonized by endocardial cells of the AV and OFT when these cells undergo epithelial to mesenchymal transformation. Endocardial cushions serve a sphincter-like function (de Jong et al. 1992; Barry 1948) until valve development occurs in specific regions within these cushions (Nomura-Kitabayashi et al. 2009). The AV endocardial cushions fuse and condense into primordial mitral and tricuspid valves that are then remodeled to form the valve leaflets. The distal outflow tract cushions are remodeled into the semilunar valve leaflets. More than 100 genes have been identified to play a role in this process (Savagner 2001; Lakkis and Epstein 1998; Ma et al. 2005), yet the specific role of hemodynamics in valvular development remains unclear. Hemodynamic forces are clearly essential, as several groups have shown that experimentally perturbed flows lead to pronounced valvular defects (Hogers et al. 1997, 1999; Ursem et al. 2004). Further, it has long been known that valve-like structures can be formed under specific hemodynamic conditions in artificial flow models of the developing heart, which was cleverly shown by placing putty in a tube under flow to illustrate the transformation of cushions into valve-like structures (Rodbard 1956). More recent work shows that contracting cardiac myocytes as well as reversing flow are required for leaflet formation (Goodwin et al. 2005; Biechler et al. 2010; Vermot et al. 2009). Whether hemodynamic forces alone are sufficient to shape a cushion into a valve leaflet remains unknown.

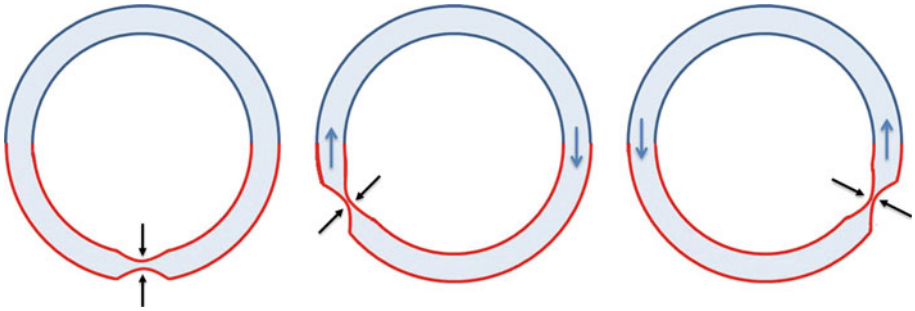

Fig. 2 Closed loop tube filled with liquid, consists of a stiff section (*blue*) and a soft section (*red*). Periodic compression (*black arrows*) at an asymmetric site of the soft tube section leads to unidirectional flow, while at the symmetric site no flow is generated. The flow direction (*blue arrows*) depends on the compression site. This figure has been motivated by the illustration presented in Manner et al. (2010)

3 Mechanics of early pumping

Several stages prior to septation and valve formation, the early tubular heart beats and pumps blood. The pumping mechanism of the valveless, tubular heart is not yet clear and is currently an active research field. There is a controversy among scientists focusing on two main theories on early embryonic valveless pumping, namely the peristaltic pumping and the Liebau effect pumping. Initially, it was assumed that the heart pumps blood through peristaltic motion, in which a contraction wave, generated by activation of myocardial cells, travels along the tubular heart causing blood to flow. Observations of the embryonic tubular heart motion during the cardiac cycle were consistent with a contraction wave traveling from the sinus venosus to the atrium, the ventricle, and the outflow tract (Barry 1942). Peristalsis has also been observed in other organs, for example, the gut or gastric emptying (Kunz et al. 1998), and peristaltic pumps are widely known in engineering practice. It was not until Liebau's observations (Liebau 1954, 1957) that another widely accepted theory for valveless pumping evolved. Liebau's experiments revealed that valveless pumping can be achieved by periodically compressing a single asymmetric site of a tube (with no need for a traveling active contraction wave). The Liebau pump is also referred to as a suction or impedance pump. Liebau's extensive experimental work on valveless pumping utilized closed loop tubes made of stiff and soft elastic sections filled with liquid, as well as straight open elastic tubes laying in a liquid-filled bath. In both cases, periodical compression at an asymmetric site (in the soft elastic section) leads to unidirectional flow (e.g., see Fig. 2). Similar experiments were conducted by numerous researchers to understand the principles of valveless pumping and to identify the pumping mechanism in the developing heart. Flow rate and direction of the flow were shown to be nonlinearly dependent on the compression frequency and duty cycle (Kenner et al. 2000; Moser et al. 1998; Ottesen 2003; Kilner 2005). An attempt to explain the cause of net flow was provided based on the compliance, wave propagation, and reflection caused by impedance mismatch (Hickerson et al. 2005; Hickerson and Gharib 2006). Experimental observations, together with analytical and computational models (see later section on modeling), provided valuable information on basic mechanisms of valveless pumping. However, a complete understanding of all the physical interactions that drive valveless pumping remains elusive.

There is still controversy among researchers as to whether the developing heart works as a peristaltic or impedance pump. After studying the embryonic zebrafish heart motion, Forouhar et al. (2006) concluded that it works as an impedance pump. However, other researchers disagree with this conclusion (Manner et al. 2010). They acknowledged that biological peristaltic pumps are likely more complex than simple technical peristaltic pumps in an engineering sense [e.g., the roller pump, in which rotating rollers cause the periodic deformation required for pumping (Usha and Rao 1995)] and that arguments presented by Forouhar et al. (2006) in support of impedance pumping are valid only when the comparison of pumping mechanisms relies on observations in impedance pumps versus technical peristaltic pumps. To settle this controversy, it would be necessary to determine whether the tubular heart experiences active contraction throughout the myocardial layer (along the whole heart), as in a peristaltic pump, or if this contraction wave is triggered from a single compression site, as in the impedance pump. In support of peristaltic pumping in the biological sense, there seems to be a functioning conduction system in the embryonic heart as early as 48 h of incubation, which is apparent through atrioventricular heart blocks when exposing the embryonic hearts to ouabain and digitalis solutions (Paff and Johnson 1938; Paff 1940; Paff et al. 1964). We note that the embryonic chick heart at stage HH18 deviates significantly from the tubular geometry due to the growth of trabeculae, which needs to be taken into consideration when studying the pumping mechanism of embryonic hearts. Further, it has been observed that upon myocardial contraction, endocardial cushions occlude the lumen completely, while impedance

pumping would predict full occlusion of the lumen only at a single compression site (Manner et al. 2010). Despite these findings, the controversy is not settled. The mechanism of valveless pumping in the developing heart may not be purely based on impedance or peristaltic pumping but rather a combination of both pumping mechanisms (Manner et al. 2010), and this mechanism might change over developmental stages. A thorough review on the mechanics of early pumping is given by Manner et al. (2010), where an in-depth discussion on the impedance pump versus the peristaltic pump is provided. More research in this fascinating area is needed to better understand how the developing tubular heart functions, and the biomechanical implications of this.

4 Normal physiological changes in the heart over early developmental stages

During early stages of development, cardiac physiology changes quickly; pressure and cardiac output increase exponentially to satisfy the growing demands of the embryo, and rapid structural changes alter the patterns of flow. Developmental changes in stroke volume, pressure, and cardiac rate have been measured primarily in chick, but also in mouse, Xenopus (frog), and zebrafish embryos. These physiological changes are described below and summarized in Table 2.

4.1 Cardiac rate

The embryonic chick heart starts beating after about 30 h of incubation (~HH10), even before blood circulation starts, which occurs around HH11 (Faber et al. 1974). The cardiac rate of embryonic chick hearts has been quantified using different methods. The easiest way to determine cardiac rate at early stages of development, when the embryo tissues are semitransparent, is through visual counting under the microscope (Cohn 1928; Parpart and Glaser 1929). Electrocardiogram measurements to determine cardiac rates in chick embryos have also been performed from 1 to 19 days of incubation (Bogue 1932). Cardiac rate can alternatively

Table 2 Hemodynamic parameters of the normal embryonic heart

Physiological parameter	Animal study	Developm. range	Parameter range	Reference
Stroke volume (mm^3)	Chick	HH12–HH29	0.01 ± 0.003–0.69 ± 0.03	Hu and Clark (1989)
	Chick	HH16–HH21	0.06 ± 0.01–0.13 ± 0.02	Keller et al. (1994)
	Xenopus Laevis	3 mg–1 g	0.0024–7.6	Hou and Burggren (1995)
	Chick	HH21–HH27	0.149 ± 0.017–0.67 ± 0.031	Lucitti et al. (2005)
	Chick	HH24	0.43 ± 0.03	Benson et al. (1989)
CO (mm^3/min)	Chick	HH12–HH29	1.2 ± 0.24–144 ± 6	Hu and Clark (1989)
	Xenopus Laevis	3 mg–1 g	0.25–623	Hou and Burggren (1995)
	Zebrafish	1 dpf–4 dpf	0.04–0.081	Jacob et al. (2002)
PSVP (mmHg)	Chick	HH12–HH29	0.95 ± 0.04–3.45 ± 0.1	Hu and Clark (1989)
	Mouse	E9.5–E14.5	2.13 ± 0.3–11.15 ± 0.54	Ishiwata et al. (2003)
	Zebrafish	5 dpf–3 mpf	0.47 ± 0.09–2.49 ± 0.25	Hu et al. (2000)
EDVP (mmHg)	Chick	HH12–HH29	0.24 ± 0.02–0.82 ± 0.03	Hu and Clark (1989)
	Chick	HH16–HH21	0.20 ± 0.02–0.34 ± 0.03	Keller et al. (1994)
	Mouse	E9.5–E14.5	0.43 ± 0.10–0.88 ± 0.08	Ishiwata et al. (2003)
	Zebrafish	5 dpf–3 mpf	0.08 ± 0.07–0.27 ± 0.10	Hu et al. (2000)
SW (mm^3 mmHg)	Chick	HH12–HH29	0.003 ± 0.0015–1.042 ± 0.046	Hu and Clark (1989)
	Chick	HH21	0.44 ± 0.03	Stekelenburg-de Vos et al. (2005)
	Chick	HH16–HH21	0.05 ± 0.01–0.22 ± 0.03	Keller et al. (1994)
Cardiac rate (BPM)	Chick	HH12–HH29	103 ± 2–208 ± 5	Hu and Clark (1989)
	Chick	HH16–HH24	90 ± 7–130 ± 13	Keller et al. (1991)
	Mouse	E10.5–E14.5	124.7 ± 5.2–194.3 ± 13.2	Keller et al. (1996)
	Mouse	E10.5–E14.5	158.5 ± 10.0–224.7 ± 14.8	Ishiwata et al. (2003)
	Xenopus Laevis	3 mg–1 g	116–89	Hou and Burggren (1995)
	Zebrafish	5 dpf–1 mpf	105.1 ± 6.1–129.6 ± 11.4	Hu et al. (2000)
	Zebrafish	1.5 dpf–4 dpf	135–175	Pelster and Burggren (1996)

EDVP end-diastolic ventricular pressure, *PSVP* peak systolic ventricular pressure, *E* embryonic days in mice, *SW* stroke work, *CO* cardiac output, *BPM* beats per minute, *dpf* days post-fertilization, *mpf* months post-fertilization

be quantified from arterial or ventricular pressure measurements (Hu and Clark 1989; Hochel et al. 1998). A comparison of the cardiac rates in the literature (Benson et al. 1989; Hu and Clark 1989; Keller et al. 1991; Cuneo et al. 1993; Keller et al. 1996; Ishiwata et al. 2003) reveals that at the same developmental stages, reported cardiac rates vary widely. These differences are most likely the result of different temperatures and the invasive nature of some of the techniques employed. Nevertheless, studies concluded that cardiac rate in the early embryonic chick hearts and mice increase roughly linearly with developmental stage (Cuneo et al. 1993), while it decreases for the larvae of Xenopus laevis (Hou and Burggren 1995) (see Table 2). Why these observed differences are inherent is not well understood and awaits an explanation.

4.2 Stroke volume and embryo weights

Stroke volume is the volume of blood ejected by the ventricle in one cardiac cycle. Stroke volume increases rapidly throughout developmental stages as the embryo grows (Hu and Clark 1989; Keller et al. 1994). It can be estimated either by measuring blood flow in the dorsal aorta (Hu and Clark 1989) or from the difference between end-diastolic and end-systolic ventricular volume (Faber et al. 1974; Keller et al. 1994). Stroke volume normalized by embryonic body weight slightly decreases with body weight (slope of regression line is $-0.2\,\mu L/mg^2$, $r^2 = 0.55$) throughout early developmental stages (HH12–HH29) for the chick embryo (Hu and Clark 1989; Hou and Burggren 1995), while it slightly increases with body weight (slope of regression line is $0.4\,\mu L/mg^2$, $r^2 = 0.66$) for the larvae of Xenopus (Hou and Burggren 1995). Similarly, the cardiac output (mean circulating volume of blood per minute) normalized by embryonic body weight is approximately constant throughout early developmental stages for the chick embryo (Clark et al. 1986; Hu and Clark 1989), while it increases with body weight (slope of regression line is $0.36\,\mu L/min\,mg^2$, $r^2 = 0.61$) for the larvae of Xenopus (Hou and Burggren 1995). The mentioned behavior for the cardiac output occurs even though the cardiac rate increases in chick twofold, while the stroke volume increases by a factor of 70 from HH12 to HH29; for the larvae of Xenopus, the cardiac rate decreases, while the stroke volume increases by a factor of more than 3,100 from 3 mg to 1 g body weight (see Table 2). These studies suggest that the stroke volume plays a primary role and the cardiac rate a secondary role to promote blood flow in the growing embryo.

Embryonic ventricle wet weight increases with developmental stages in chick embryos (Clark et al. 1986). However, the relative weight of the ventricle to embryo weight decreases by a factor of 20 from HH18 to HH43, the final stage before hatching. Similarly for the zebrafish, the relative weight of the ventricle to embryo weight decreases from 0.11 at 48 h of post-fertilization to 0.02 in an adult stage (Hu et al. 2000). This may be an indicator of a more efficient pumping mechanism of the mature heart than the embryonic heart.

4.3 Ventricular pressure

Ventricular blood pressure increases exponentially over developmental stages. Embryonic pressure measurements are usually performed with a servo null system, by inserting a micro-pipette in the heart. Ventricular pressures have been measured extensively to characterize cardiac function in the embryonic heart (Clark et al. 1986; Hu and Clark 1989; Keller et al. 1991; Chabert and Taber 2002; Ishiwata et al. 2003). As in the mature heart, the end-diastolic ventricular pressure, which is the pressure just before cardiac contraction, and peak systolic ventricular pressure, which is the maximum pressure achieved during contraction, are of key importance and have been quantified in embryos over developmental stages (see Table 2). It was observed that the time difference between end-systole and peak ventricular pressure increases with developmental stages in chick embryos (HH16 to HH24), which may be the result of a change in vascular impedance with embryonic growth (Keller et al. 1991). In both chick and mouse ventricles, it has been found that peak systolic pressures increase faster than end-diastolic pressure over early developmental stages (Clark et al. 1986; Hu and Clark 1989; Ishiwata et al. 2003), giving rise to higher stroke volumes. Pressure pulsatility, the difference between peak systolic and end-diastolic blood pressure, therefore increases over developmental stages, which may have consequences for cardiac growth in response to loading.

The stroke work, the work the ventricle performs to enable blood circulation in the cardiovascular system, is an important physiological parameter that can be easily determined from the integral of ventricular pressure over ventricular volume during a cardiac cycle. Alternatively, the stroke work has been estimated as the mean arterial pressure times the stroke volume, observing an exponential increase from HH12 to HH29 (Hu and Clark 1989). The measured increase in stroke work suggests an increase in the number and reorganization of the myocardial cells.

4.4 Pressure–volume loops

The pressure–volume (PV) loop of the mature heart is determined from pressure and volume measurements of the left ventricle over one cardiac cycle. Ventricular PV loops characterize cardiac function, including the diastolic filling phase and the systolic contraction phase. They are also used to quantify stroke volume, stroke work (defined as the area enclosing the pressure volume curve), left ventricular end-diastolic volume (often used as a representative measure of preload), ventricular contractility, afterload (contraction

Table 3 Physiologic parameters for altered hemodynamics of the embryonic chick heart

Physiological parameter	HH stage	Hemodyn. intervention	Parameter range	Reference
Stroke volume (mm^3)	HH21–HH27	LAL (1–30 HR)	0.067 ± 0.007–0.662 ± 0.039	Lucitti et al. (2005)
	HH16–HH21	1–2 μL infusion	0.1 ± 0.01–0.23 ± 0.04	Keller et al. (1994)
	HH24	PI150	0.19 ± 0.03	Benson et al. (1989)
SW (mm^3 mm Hg)	HH16–HH21	1–2 μL infusion	0.08 ± 0.02–0.33 ± 0.04	Keller et al. (1994)
	HH21	Venous clip	0.42 ± 0.03	Stekelenburg-de Vos et al. (2005)
EDVP (mm Hg)	HH16–HH21	1–2 μL infusion	0.30 ± 0.02–0.48 ± 0.02	Keller et al. (1994)

SW stroke work, *HR* hours of reincubation, *LAL* left atrial ligation, *EDVP* end-diastolic ventricular pressure, *PI150* pacing at intrinsic cardiac rate of 150 %. See also Table 2 for normal values

force developed in the wall of the ventricle during blood ejection), and ventricular elastance (the slope of the PV curve during diastole).

Pressure-area loops (rather than pressure–volume loops) have been initially measured in embryonic chick from HH16 to HH24 using optical images of the beating heart and simultaneous pressure measurements (Keller et al. 1991). This is because 2D optical images of the heart provide the means to readily determine ventricular area in the imaging plane, rather than ventricular volume. Using data from pressure-area loops, it was found that the maximum ratio of ventricular pressure to area represented the end-systolic cardiac phase better than either peak ventricular pressure or minimum ventricular area. This work on pressure-area loops was subsequently extended to PV loops (Keller et al. 1994; Stekelenburg-de Vos et al. 2005), where the volume was estimated from 2D images of the heart ventricle assuming an ellipsoidal ventricular shape. Despite the lack of valves and proper chamber formation in the early developing heart, PV loops in the tubular heart resemble those in the mature heart and have therefore been used extensively to characterize embryonic cardiac function.

5 Effect of physiological alterations on cardiac development

Ablation or overexpression of genes predicted to affect cardiac development leads to high embryo mortality and widespread physiological and morphological defects (Kirchhoff et al. 2000; Grossman et al. 2011). Environmental and mechanical interventions are commonly used to assess the specific effects of changes in hemodynamics. Numerous investigators have studied the acute and chronic effects of altered blood flow in the embryonic circulation using a combination of microsurgical and microscopic techniques.

Temperature variations lead to dramatic changes in cardiac rate in embryonic chicken, limulus, and fundulus larvae (Cohn 1928; Parpart and Glaser 1929; Cuneo et al. 1993; Phelan et al. 1995; Glaser 1929; Crozier and Stier 1927). Increasing temperature leads to an increase in cardiac rate and a decrease in stroke volume (Cuneo et al. 1993; Phelan et al. 1995). Similarly, an increase in cardiac rate achieved by pacing also reduces stroke volume (Benson et al. 1989) (see Table 3). Injection of saline or plasma leads to a transient increase in preload (Keller et al. 1994) and a maintained, linear increase in stroke volume (Faber et al. 1974; Wagman et al. 1990) (see Table 3). Together these data suggest that the change in stroke volume due to pacing or temperature variations is due to altered diastolic filling time, affecting ventricular preload.

More recently, cardiac malformations resulting from alterations in blood flow at early stages have been extensively studied with surgical intervention procedures in chicken embryos. Chick development in ovo provides easy access to the hearts for microsurgical manipulation. The cardiovascular system quickly remodels to adapt to new flow conditions by adjusting the volume of circulating blood and intravascular pressure. However, the adjustment to altered mechanical loads results in changes in myocardial size, architecture and function (Sedmera et al. 1999; Tobita and Keller 2000), cardiomyocyte proliferation (Sedmera et al. 2002), and conduction system maturation (Reckova et al. 2003) as well as a spectrum of atrioventricular anomalies which closely resemble defects found in human patients with congenital heart disease (Hogers et al. 1997, 1999). The most commonly performed interventions in chick embryos are discussed below and representative altered physiological parameters due to hemodynamic changes in the chick embryo are listed in Table 3.

Venous clipping or ligation of vitelline vein Designed to test the effect of reduced placental blood flow on embryonic heart development, in this model the right lateral vitelline vein, which drains the right side of the yolk sac vasculature, is ligated. This ligation forces blood to re-route through the caudal capillary plexus and into the left lateral vitelline vein. Thus, venous return is altered and blood flow is acutely reduced (Stekelenburg-de Vos et al. 2003). This

temporarily decreases mechanical load on the myocardium and, importantly, leads to shifted blood flow patterns through the heart from the inner to outer curvature (Hogers et al. 1997). After 24 h, stroke volume and dorsal aortic blood flow return to normal levels (Stekelenburg-de Vos et al. 2005; Ursem et al. 2004); however, the transient decrease in load leads to impaired looping (Broekhuizen et al. 1999) and a spectrum of outflow tract, ventricular septal, and valvular defects (Hogers et al. 1997, 1999; Ursem et al. 2004). Reduced ventricular contractility, derived from pressure–volume loops during venous hemorrhage, suggests that the hemodynamic perturbations cause long-term and likely permanent effects (Stekelenburg-de Vos et al. 2005; Ursem et al. 2004).

Outflow tract banding (OTB) Designed to test the effect of increased ventricular afterload, in OTB a suture is placed around the outflow tract and tightened to reduce the cross-sectional area of the outflow tract lumen (Clark et al. 1989; Tobita and Keller 2000; Tobita et al. 2002; Sedmera et al. 1999). This loads the ventricle increasing intra-ventricular pressure. As a result, blood velocities through the outflow tract are elevated, increasing shear stress at the wall (Rugonyi et al. 2008). Banded hearts must work harder; therefore, they become enlarged with a thicker compact myocardium and increased contractile force (Sedmera et al. 1999; Miller et al. 2003). The trabeculae also develop to be thicker and more spiraled (Sedmera et al. 1999). Together these findings suggest a ventricular wall that has permanently adapted to the elevated load by enhancing cardiac contraction and becoming less compliant.

Left atrial ligation or clipping (LAL) LAL has long been used as a model of human hypoplastic left heart syndrome (Rychter et al. 1979; Rychter and Rychterova 1981), a group of congenital cardiac anomalies characterized by underdevelopment of the left side of the heart (Friedman et al. 1951). A suture or clip is placed around the left atrium, decreasing atrial volume and cardiac output, and transiently increasing cardiac rate. Hemodynamic parameters seem to normalize at later developmental stages (14–32 h after LAL) (Lucitti et al. 2005). A similar effect can be achieved via mechanical obstruction of the left AV orifice (Harh et al. 1973). The reduced left ventricular volume load (preload) in LAL hearts leads to underdevelopment of left heart structures, left ventricular hypoplasia, decreased stroke volume and cardiac output, decreased proliferation, augmented trabecular compaction, and increased wall stiffness (Sedmera et al. 1999; Tobita and Keller 2000; Sedmera et al. 2002; Lucitti et al. 2005). Despite these widespread hemodynamic changes, arterial pressure is maintained via adjustments in compliance and impedance (Lucitti et al. 2005). Reversal of left ventricular hypoplasia induced by LAL can be achieved, to some degree, with right atrial clipping. de Almeida et al. (2007) showed that right atrial clipping increases ventricular preload, countering the effects of LAL, and leads to restored myocardial volume and increased proliferation on the left side of the heart.

Other interventions Banding, ligation, and clipping procedures lead to widespread changes in hemodynamics. In an effort to elucidate how even microscale changes in tissue geometry can affect hemodynamics and subsequent development, Yalcin et al. (2010) used local, targeted photoablation in the chick combined with 2-photon microscopy. Ablation of an area on the AV cushion of HH24 chick embryos led to acute changes in cardiac output and flow velocity, as well as AV regurgitation. Within 48 h, these hemodynamic changes led to left atrial dilation, and arrested both ventricular and trabecular growth. The size of tissue ablated (radius ∼100 microns) was quite large relative to the chick heart size at that stage (e.g., outflow tract radius at that stage ∼200 microns (Keller et al. 1990)). However, the microscale perturbation concept and photoablation technology appear promising.

Other model systems The chick is not the only model in which flow can be manipulated for the study of early heart development. Over the last decade, the zebrafish has arisen as a new model organism. This is largely due to the ability to perform forward genetic screens, allowing for the identification of genes important for cardiovascular development, and various reverse genetic approaches (e.g., morpholinos) (Bakkers 2011). Indeed, such genetic alterations have led to numerous cardiac phenotypes with widespread perturbations (Miura and Yelon 2011). Furthermore, the external development and transparency of zebrafish embryos provide optical access to the embryonic heart for various manipulation and imaging techniques. For example, Hove et al. (2003) prevented intracardiac blood flow by implanting beads into the zebrafish inflow or outflow tract. Laser scanning, confocal microscopy, and digital particle image velocimetry revealed reduced blood flows in bead-implanted embryos and drastically reduced shear forces (∼tenfold). These changes led to an abnormal third chamber, impaired looping, a lack of endocardial cushion formation, and delayed peristaltic heart contraction, thus clearly illustrated the effect of hemodynamic forces on heart development.

Frogs have long been used to study heart development due to their external development and, in the case of Xenopus, their large egg size. More recently, microinjection techniques for over-/mis expression of a gene or loss of function approaches have made the frog a powerful model for regulation of transcription and cell signaling in the developing heart (Warkman and Krieg 2007). A *Xenopus tropicalis* model with a mutation in cardiac myosin (lacking myh6 protein) exhibits an absence of myofilaments, sarcomeres,

and contractility (Abu-Daya et al. 2009), and thus these embryos develop without any effects of pressure load or shear stress. Surprisingly, both looping and chamber formation are approximately normal, whereas trabeculation and valve formation is entirely absent. This is remarkably similar to a mutant axolotl, *Ambystoma mexicanum*, salamander. When homozygous for the recessive cardiac lethal gene c, these cardiac mutants exhibit deficient sarcomere formation, and a complete lack of contractility and trabeculation (Fransen and Lemanski 1988). Whether the trabecular and valve defects observed in *Xenopus tropicalis* and axolotl mutants are due to the lack of gene function or the lack of hemodynamic forces is as yet unknown. Similar *Xenopus tropicalis* models with reduced cardiac function (Goda et al. 2006) have yet to be characterized and may better elucidate the effects of hemodynamic forces on heart development in the frog.

6 Modeling heart development

The hemodynamic forces that modulate cardiac growth and remodeling vary between developmental stages, but due to cardiac wall motion and morphology, these forces also vary tremendously within the heart segments and over the cardiac cycle. To better understand the complexity and the role of biomechanical forces on gene expression, cardiac growth and remodeling, and cardiac pumping, several computational models of the developing heart have been developed and implemented. These models address diverse questions, and range from simplified models to understand fundamental issues to models that use embryo-specific cardiac geometries, obtained from in vivo high-resolution imaging techniques, which also include cardiac wall motion and blood pressure pulsatility. All these models, from the simplest to the more sophisticated, greatly contribute to our understanding of biomechanics at early stages of development.

6.1 Models of valveless pumping

The Liebau effect provides a model for valveless pumping of the embryonic heart. Unfortunately, the underlying physics that drive unidirectional flow are quite complex and not well understood. Thus, mathematical and computational models have been developed and analyzed with different levels of complexity. Models that accounted for an impedance pump in a closed circular tube include (i) a 2D computational model of the pump, in which flow is modeled using the Navier–Stokes equations and the immersed boundary method is used to account for the interaction between the fluid and the tubing (Jung and Peskin 2001); (ii) a simplified, discrete mathematical model of the pump in which compliance as well as fluid resistance and inertia were accounted for (Jung 2007); and (iii) a one dimensional set of equations derived from the Navier–Stokes equations, representing the pump (Ottesen 2003). All these models accounted for differences in stiffness between tubing sections in the impedance pump, which is key to achieve flow. Because of the different levels of complexity and details in those models, as well as the focus of the modeling efforts, these models complementary showed different characteristics of impedance pumping. The models revealed that flow direction depends nonlinearly on the frequency and the amplitude of the compression excitation, but also on the tube stiffness, with switch in flow direction occurring at multiple frequencies (Jung and Peskin 2001; Ottesen 2003; Jung 2007). Further, these models showed that the frequency at which peak average flow occurs depends on the tube radius and stiffness, as well as fluid density (Jung 2007). The peak average flow increases with larger differences in the elasticity modulus between the stiff and soft parts of the tubing, and with the excitation source closer to the soft/stiff tube intersection (Ottesen 2003). Another main observation was that average flow increases with increasing compression ratios at the same peak frequency (Ottesen 2003). The discussed models, however, did not intend to properly represent the embryonic heart tube, but rather to understand the underlying mechanism of the impedance pump.

Other works utilized models of the impedance pump that resembled the early embryonic heart more accurately. In Avrahami and Gharib (2008), an open straight tube with finite thickness is modeled for the numerical analysis of the Liebau effect, with the fluid structure interaction problem solved using the Navier–Stokes equations for the fluid and direct coupling of the tubing walls. The model reproduced experimental results reported in Hickerson et al. (2005) for average flow versus the location of the contraction 'pincher' and duty cycle and found that average flow increases with increasing compression rate as observed by Ottesen (2003). The study further concluded that the interaction of reflected waves is the driving force for average unidirectional flow. In an extension to this work, the tube was modeled with two distinct layers of stiffness and thickness motivated by the stiff myocardial layer and the soft cardiac jelly in the embryonic heart (Loumes et al. 2008). Simulations of the model showed that an off-centered periodic compression of the external wall with relatively small amplitude generates significant amounts of unidirectional flow, suggesting that the morphology of the embryonic heart (with distinct tissue layers) is optimal for valveless pumping.

To study the effect of cardiac cushions on peristaltic valveless pumping, a simplified 2D model of the heart was developed by Taber et al. (2007), in which a wave-like displacement was prescribed along the wall to represent active contraction of the myocardial wall. The model revealed that without cushions, fluid velocity achieved inside the heart is relatively moderate, and flow pressure oscillates smoothly. In contrast, when cushions are present, flow velocity exceeds

the prescribed wave speed, and pressure oscillations increase sharply. The study thus revealed that cardiac cushions are essential for blood pulsatility in the early developing heart and that wall shear stress on cardiac cushions is distinct from those in the rest of the heart, which suggests that the distribution of wall shear stresses may play an important role in valve development.

While the described models reveal interesting aspects of valveless pumping and their application to the embryonic heart, none of these models fully support arguments in favor of peristaltic nor impedance pumping in the developing heart. Features from both impedance and peristaltic pumping have been observed in the developing heart, and actual pumping in the tubular heart is more complex than the models presented up to date. Nevertheless, the models provide a means to understand the basics of the pumping mechanism in the developing heart.

6.2 Models of wall stress and growth in the developing heart

Studies to characterize the developing cardiac wall mechanics, including the mechanical properties of cardiac tissue, have been performed on chick embryos. In those studies, ventricular pressure was recorded, while the heart was imaged with a CCD camera. To characterize cardiac function, pressure–volume loops were extracted from the simultaneous pressure and imaging data (Keller 1998; Keller et al. 1991; Hu et al. 1991). Further, by placing micro-spheres on the myocardium of the developing heart ventricle, and following the motion of the micro-spheres over time (by analyzing image recordings from the CCD camera), myocardial strains were calculated. From measurements of micro-sphere motions, then pressure-strain and stress-strain curves for the myocardium of the developing heart ventricle were obtained (Tobita et al. 2002; Tobita and Keller 2000; Ling et al. 2002). These methods yielded good approximations of the mechanics of the developing heart.

Biomechanical models of the developing heart (Taber and Humphrey 2001) have generally focused on quantifying stresses on the walls of the ventricle. Modeling studies also considered the effects of wall stress on cardiac growth (Taber and Humphrey 2001; Lin and Taber 1995). Based on the work of Rodriguez et al. (1994), Lin and Taber (1995) modeled cardiac growth using a growth deformation gradient tensor to describe cardiac tissue growth. In their model, the heart grows when wall stress is larger than a 'growth-equilibrium' stress. When the growth model was applied to a simplified cylindrical model of the developing heart ventricle, volumetric (mass) growth of the developing ventricle from HH21 to HH29 was reproduced. Kowalski et al. (2012) provides a new model to predict aortic arch formation based on the outflow tract orientation and the associated alterations in hemodynamics. An extensive review of embryonic growth models is provided therein as well.

As noted by Lin and Taber (1995), and documented in several studies (Hu and Clark 1989; Clark et al. 1989), intracardiac pressure increases as development progresses; thus, stresses in the heart also increase with development. Growth models that apply for mature systems therefore do not apply during development, as there is no homeostatic state to which cells might try to recover. Growth models must account for changes in the growth-equilibrium stress that occur with cardiac development; otherwise, the heart would not grow and might reduce in size initially, when the wall stress is low, or it might not stop growing if the wall stress becomes larger than the growth-equilibrium stress after reaching some developmental stage. More research is sorely needed in this area to understand how the heart adapts to and grows in response to ever changing pressure cues.

6.3 Models of early cardiac blood flow dynamics from reconstructed heart geometries

Several limitations in measuring blood flow velocities in the tiny, rapidly beating developing heart, with enough spatial resolution to calculate shear stresses (proportional to gradients of velocities perpendicular to the heart wall), have sparked interest in the development of computational fluid dynamics models of the heart. For example, particle image velocimetry has been used to measure blood flow velocity in the developing hearts of zebrafish (Hove 2006), mice (Jones et al. 2004), and chicks (Vennemann et al. 2006; Hierck et al. 2008). In this technique, using a high-speed imaging camera, flow markers are followed in time, and blood flow velocities are calculated from the motion of the markers, which is extremely challenging for the rapidly beating developing heart, and results in imprecise velocity gradients, and thus wall shear stresses (Hove 2006). Other groups have used Doppler ultrasound or laser Doppler velocimetry (Butcher et al. 2007; Lucitti et al. 2005; Yoshigi and Keller 1997; Phoon and Turnbull 2003; Rugonyi et al. 2008; Ma et al. 2010). An important limitation of Doppler techniques (including Doppler OCT), however, is that the measured velocities are projections of the 3D velocity vector in the direction of the Doppler probe (1D velocity component). Therefore, precise information about the 3D orientation and magnitude of velocity can only be estimated (see e.g., Fig. 3). To overcome these drawbacks, many groups have resourced to computational models of blood flow dynamics within the developing heart.

Computational models have been used to characterize blood flow and wall shear stress patterns in the developing chick heart. Most of these studies assumed blood to be Newtonian and used a static heart geometry. Using idealized geometrical representations of the heart, effects of

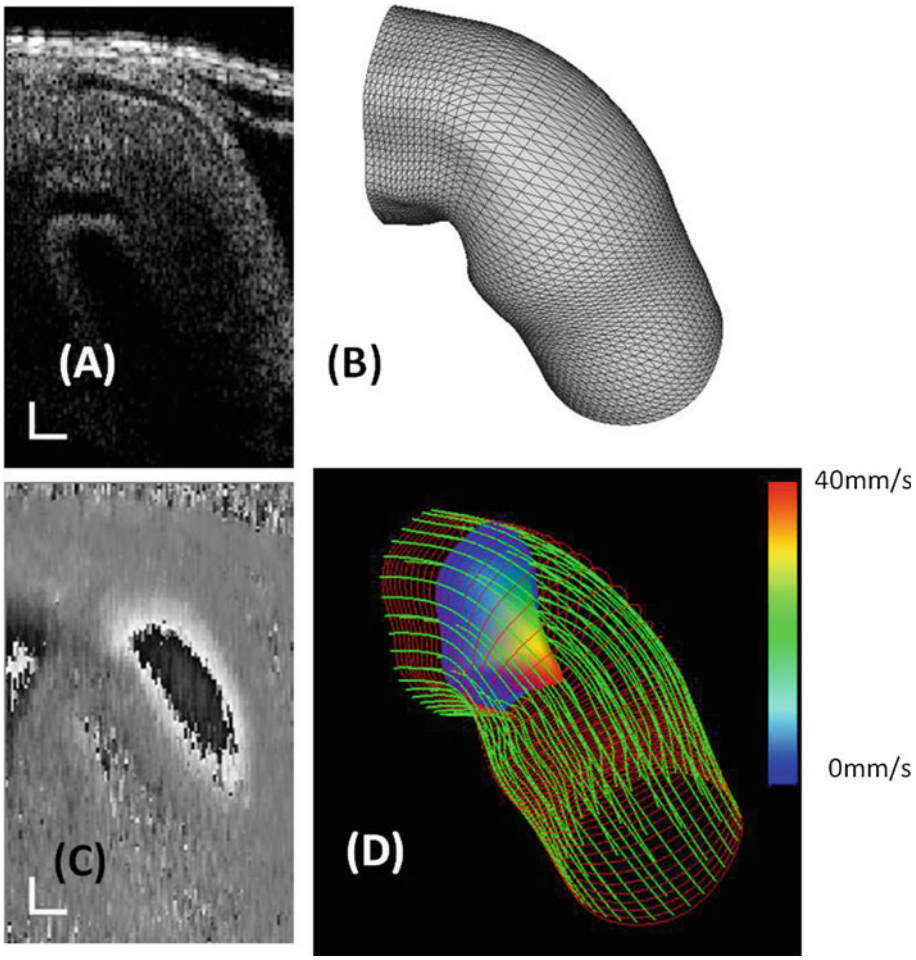

Fig. 3 Analysis of a 4D OCT image data set of the HH18 chick heart outflow tract (OFT) portion of the heart. (**A**) Structural OCT image showing a longitudinal section of the heart OFT, which connects the ventricle to the chick arterial system. (**B**) 3D structural segmentation of the OFT geometry from OCT images. (**C**) Gray scale Doppler OCT image (showing flow velocities) corresponding to the structural image shown in (**A**). (**D**) 3D blood flow reconstruction, showing flow through the inlet portion of the OFT. *Scale bar* 20 microns

curvature on blood flow dynamics through the heart were assessed (Loots et al. 2003). DeGroff et al. (2003) pioneered the use of cardiac geometries reconstructed from fixed heart tissue sections to calculate blood flow and wall shear stresses on the inside walls of chick embryonic hearts. These models showed general features of blood flow in the developing heart, including an estimation of the balance between inertia and viscous forces. These models, however, neglected the effects of cardiac wall motion and associated blood pressure pulsatility, which generate the periodic variations in blood flow and hemodynamic forces that occur during the cardiac cycle and that are important for development.

More recently, several groups have begun to characterize the 3D structure and motion of the developing heart using high-resolution imaging data and computational fluid dynamics modeling. For example, Butcher et al. (2007) has used ex vivo high-resolution micro-computed tomography (micro-CT) data to establish quantitative structural baselines that can be used for comparison with hemodynamic experimental interventions (Butcher et al. 2007; Kim et al. 2011). Wall shear stress can be estimated by combining geometry from micro-CT images with ultrasound generated velocity profiles and computational fluid dynamics to predict flow dynamics (Wang et al. 2009; Yalcin et al. 2011). These localized estimations of flow and shear stress provide important context regarding the hemodynamic stimuli present at specific locations within the developing heart (e.g., the AV canal's inner versus outer curvature) (Yalcin et al. 2011), clearly demonstrate the prominent relationship between flow, morphology, and perfusion, and have helped to provide context for the developmental patterns of cushion formation (Yalcin et al. 2011) and the aortic arches (Wang et al. 2009). However, the static nature of these ex vivo images does not capture the motion of the wall. In vivo micro-CT imaging in the chick is still in its infancy (Henning et al. 2011) and is not likely to capture wall motion due to the chick's rapid heart rate (~2.5 Hz). Thus, there is an absence of computational models that accurately represent the dynamics of cardiac motion and blood circulation.

Optical coherence tomography (OCT) imaging has the temporal and spatial resolution needed for image

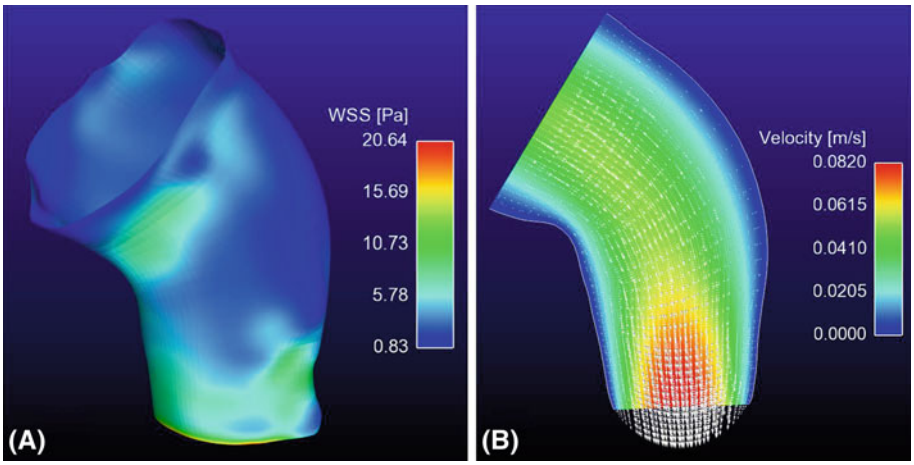

Fig. 4 Hemodynamic computational model of the HH18 chick heart outflow tract. (**A**) Wall shear stress distribution (WSS), (**B**) blood flow velocities. The heterogenous distribution of WSS and the velocity profile were obtained from the solution of the computational fluid dynamics problem with pressure boundary conditions and no slip condition at the outflow tract wall. For visualization purposes, we present the velocity profile along a plane passing through the centerline of the outflow tract

acquisition of the early embryonic chick, quail, and Xenopus hearts (Fujimoto 2003; Tomlins and Wang 2005; Jenkins et al. 2007a). Because the heart tissue layers have different optical properties, OCT allows in vivo imaging of internal cardiac microstructures, where the myocardium, cardiac jelly, and endocardium/lumen can be distinctly identified (Jenkins et al. 2007b; Rugonyi et al. 2008). Using 4D (3D + time) reconstructed images of the chick heart outflow tract at HH18, Liu et al. (2011) developed and implemented a computational fluid dynamics model (see e.g., Fig. 4) that includes wall motion and blood pressure pulsatility, as well as fluid inertia. This model has the advantage that the heterogeneous distribution of the wall shear stresses, which is important for proper cardiac development, can be temporally and spatially quantified. The study found that wall shear stresses are maximal during the ejection phase and are more elevated in the outflow tract outer curvature and regions where cardiac cushions protrude. Undoubtedly, computational models of hemodynamics and tissue motion of the whole developing heart will soon enable accurate quantification of the biomechanical environment to which cardiac cells are subjected over the cardiac cycle and developmental stages, both under normal and altered hemodynamic conditions.

The fluid dynamics aspects in context to the early developing embryo are exhaustively reviewed and discussed by Santhanakrishnan and Miller (2011). Biomechanical modeling of the embryonic heart is an emerging field which will certainly grow in the years to come. To further elucidate the mechanisms by which hemodynamic forces affect heart development, quantification of these forces is necessary. Thus, biomechanical modeling approaches, in combination with physiological and molecular biology quantifications, will surely be critical to advancing our understanding of embryonic hemodynamic causes of congenital heart disease.

7 Summary

During development, the heart is constantly adapting to the growing demands of the embryo and cardiac cells experience the effects of ever increasing pressures and volume flow rates. Much is known about the physiology of the developing heart and the morphological changes it experiences under normal and altered conditions. Details of structural anomalies have been reported by numerous groups. More recently, advanced imaging techniques have elucidated changes in flow. Genes that are essential for cardiac development and that lead to congenital heart defects when expression is altered have been identified. Indeed, the effects of altered hemodynamic conditions on cardiac function and morphology have been well studied. However, there is still much to be learned, as the fundamental mechanisms that drive cardiac adaptation (even under normal genetic and hemodynamic conditions) are not well understood. The important role of biomechanics on cardiac development, while acknowledged, has been underappreciated for many years. Fortunately, studies demonstrating that hemodynamic alterations can reproduce a number of human congenital heart defects have sparked renewed interest in the developmental cardiac biomechanics field.

Going forward, it will be critical to study the short- and long-term effects of hemodynamic alterations. Heart-wide level changes in structure and function have been well established, but there is a paucity of information at the cellular and molecular levels, in particular information pertaining to gene expression changes driven by hemodynamic forces. Links and relationships between gene expression and specific hemodynamic stimuli need to be established to better understand how differential hemodynamic stimuli could lead to differential gene expression patterns that might affect cardiac morphology and cardiac function. It will also be important to assess the timing of gene expression changes. If gene expression is permanently altered, then there are strong implications

for fetal programming. No doubt the effect of such hemodynamic alterations on gene expression will be an emerging topic in years to come.

Biomechanical modeling of the embryonic heart is also emerging, and will undoubtedly continue to gain strength as the importance of biomechanical effects on cardiac development is more widely recognized. In addition to quantifying forces, computational models have the potential to enable a better understanding of the interaction between tissues and blood flow, and how these interactions affect cell mechanobiology and signaling. Multiscale models of cardiac development that account for effects at the tissue, cell, and molecular levels (and beyond) will surely start to emerge. Computational modeling approaches, in combination with physiological and molecular biology quantifications, will surely be critical to advancing our understanding of embryonic hemodynamic causes of congenital heart disease, and in general of the embryonic origins of cardiovascular health and disease.

Acknowledgments The authors would like to acknowledge the following funding sources: NIH R01HL094570 and NSF DBI-1052 688. The authors would also like to thank the reviewers for their valuable comments and suggestions to improve the quality of the paper.

References

Abu-Daya A, Sater AK, Wells DE, Mohun TJ, Zimmerman LB (2009) Absence of heartbeat in the *Xenopus tropicalis* mutation muzak is caused by a nonsense mutation in cardiac myosin myh6. Dev Biol 336(1):20–29

Avrahami I, Gharib M (2008) Computational studies of resonance wave pumping in compliant tubes. J Fluid Mech 608:139–160

Baker K, Holtzman NG, Burdine RD (2008) Direct and indirect roles for nodal signaling in two axis conversions during asymmetric morphogenesis of the zebrafish heart. Proc Natl Acad Sci USA 105(37):13924–13929

Bakkers J (2011) Zebrafish as a model to study cardiac development and human cardiac disease. Cardiovasc Res 91(2):279–288

Barry A (1942) The intrinsic pulsation rates of fragments of the embryonic chick heart. J Exp Zool 91(2):119–130

Barry A (1948) The functional significance of the cardiac jelly in the tubular heart of the chick embryo. Anat Rec 102(3):289–298

Bartman T, Hove J (2005) Mechanics and function in heart morphogenesis. Dev Dyn 233(2):373–381

Benson JDW, Hughes SF, Hu N, Clark EB (1989) Effect of heart rate increase on dorsal aortic flow before and after volume loading in the stage 24 chick embryo. Pediatr Res 26(5):438–441

Biechler SV, Potts JD, Yost MJ, Junor L, Goodwin RL, Weidner JW (2010) Mathematical modeling of flow-generated forces in an in vitro system of cardiac valve development. Ann Biomed Eng 38(1):109–117

Bogue JY (1932) The heart rate of the developing chick. J Exp Biol 9:351–358

Bouman H, Broekhuizen M, Baasten A, Gittenberger-De Groot A, Wenink A (1995) Spectrum of looping disturbances in stage 34 chicken hearts after retinoic acid treatment. Anat Rec 243(1):101–108

Bremer JL (1932) The presence and influence of two spiral streams in the heart of the chick embryo. Am J Anat 49(3):409–440

Broekhuizen ML, Hogers B, DeRuiter MC, Poelmann RE, Gittenberger-de Groot AC, Wladimiroff JW (1999) Altered hemodynamics in chick embryos after extraembryonic venous obstruction. Ultrasound Obstet Gynecol 13(6):437–445

Bruneau BG (2008) The developmental genetics of congenital heart disease. Nature 451(7181):943–948

Burggren WW, Keller BB (1997) Development of cardiovascular systems: molecules to organisms. Cambridge University Press, Cambridge

Butcher JT, Sedmera D, Guldberg RE, Markwald RR (2007) Quantitative volumetric analysis of cardiac morphogenesis assessed through micro-computed tomography. Dev Dyn 236(3):802–809

Chabert S, Taber LA (2002) Intramyocardial pressure measurements in the stage 18 embryonic chick heart. Am J Physiol-Heart C 282(4):H1248–H1254

Challice CE, Virágh S (1974) The architectural development of the early mammalian heart. Tissue Cell 6(3):447–462

Clark EB, Hu N, Rosenquist GC (1984) Effect of conotruncal constriction on aortic-mitral valve continuity in the stage 18, 21 and 24 chick embryo. Am J Cardiol 53(2):324–327

Clark EB, Hu N, Dummett JL, Vandekieft GK, Olson C, Tomanek R (1986) Ventricular function and morphology in chick embryo from stages 18 to 29. Am J Physiol 250(3 Pt 2):H407–H413

Clark EB, Hu N, Frommelt P, Vandekieft GK, Dummett JL, Tomanek RJ (1989) Effect of increased pressure on ventricular growth in stage 21 chick embryos. Am J Physiol 257(1 Pt 2):H55–H61

Cohn AE (1928) Physiological ontogeny: a chicken embryos. xiii. the temperature characteristic for the contraction rate of the whole heart. J Gen Physiol 11(4):369–375

Colvee E, Hurle JM (1983) Malformations of the semilunar valves produced in chick embryos by mechanical interference with cardiogenesis. an experimental approach to the role of hemodynamics in valvular development. Anat Embryol (Berl) 168(1):59–71

Crozier WJ, Stier TJ (1927) Temperature and frequency of cardiac contractions in embryos of limulus. J Gen Physiol 10(4):501–518

Cuneo B, Hughes S, Benson JDW (1993) Heart rate perturbation in the stage 17–27 chick embryo: effect on stroke volume and aortic flow. Am J Physiol 264(3 Pt 2):H755–H759

Damon BJ, Rémond MC, Bigelow MR, Trusk TC, Xie W, Perucchio R, Sedmera D, Denslow S, Thompson RP (2009) Patterns of muscular strain in the embryonic heart wall. Dev Dyn 238(6):1535–1546

de Almeida A, McQuinn T, Sedmera D (2007) Increased ventricular preload is compensated by myocyte proliferation in normal and hypoplastic fetal chick left ventricle. Circ Res 100(9):1363–1370

de Jong F, Opthof T, Wilde AA, Janse MJ, Charles R, Lamers WH, Moorman AF (1992) Persisting zones of slow impulse conduction in developing chicken hearts. Circ Res 71(2):240–250

DeGroff C, Thornburg B, Pentecost J, Thornburg K, Gharib M, Sahn D (2003) Flow in the early embryonic human heart: a numerical study. Pediatr Cardiol 24(4):375–380

Egorova A, DeRuiter M, de Boer H, van de Pas S, Gittenberger-de Groot A, van Zonneveld A, Poelmann R, Hierck B (2011) Endothelial colony-forming cells show a mature transcriptional response to shear stress. In Vitro Cell Dev B 48(1):21–29

Ettensohn CA (1985) Mechanisms of epithelial invagination. Q Rev Biol 60(3):289–307

Faber JJ, Green TJ, Thornburg KL (1974) Embryonic stroke volume and cardiac output in the chick. Dev Biol 41(1):14–21

Forouhar AS, Liebling M, Hickerson A, Nasiraei-Moghaddam A, Tsai HJ, Hove JR, Fraser SE, Dickinson ME, Gharib M (2006) The embryonic vertebrate heart tube is a dynamic suction pump. Science 312(5774):751–753

Fransen M, Lemanski L (1988) Myocardial cell relationship during morphogenesis in normal and cardiac lethal mutant axolotls, ambystoma mexicanum. Am J Anat 183:245–257

Friedman S, Murphy L, Ash R (1951) Aortic atresia with hypoplasia of the left heart and aortic arch. J Pediatr 38(3):354–368

Fujimoto J (2003) Optical coherence tomography for ultrahigh resolution in vivo imaging. Nat Biotechnol 21:1361–1367

Garita B, Jenkins MW, Han M, Zhou C, Vanauker M, Rollins AM, Watanabe M, Fujimoto JG, Linask KK (2011) Blood flow dynamics of one cardiac cycle and relationship to mechanotransduction and trabeculation during heart looping. Am J Physiol Heart C 300(3):H879–H891

Gassmann M, Casagranda F, Orioli D, Simon H, Lai C, Klein R, Lemke G (1995) Aberrant neural and cardiac development in mice lacking the erbb4 neuregulin receptor. Nature 378(6555):390–394

Glaser O (1929) Temperature and heart rate in fundulus embryo. J Exp Biol 6:325–339

Goda T, Abu-Daya A, Carruthers S, Clark MD, Stemple DL, Zimmerman LB (2006) Genetic screens for mutations affecting development of *Xenopus tropicalis*. PLoS Genet 2(6):e91

Goodwin RL, Nesbitt T, Price RL, Wells JC, Yost MJ, Potts JD (2005) Three-dimensional model system of valvulogenesis. Dev Dyn 233(1):122–129

Groenendijk B, Van der Heiden K, Hierck B, Poelmann R (2007) The role of shear stress on et-1, klf2, and nos-3 expression in the developing cardiovascular system of chicken embryos in a venous ligation model. Physiology 22:380–389

Grossman TR, Gamliel A, Wessells RJ, Taghli-Lamallem O, Jepsen K, Ocorr K, Korenberg JR, Peterson KL, Rosenfeld MG, Bodmer R, Bier E (2011) Over-expression of dscam and col6a2 cooperatively generates congenital heart defects. PLoS Genet 7(11): e1002344

Hamburger V, Hamilton HL (1992) A series of normal stages in the development of the chick embryo. 1951. Dev Dyn 195(4):231–272

Harh J, Paul M, Gallen W, Friedberg D, Kaplan S (1973) Experimental production of hypoplastic left heart syndrome in the chick embryo. Am J Cardiol 31(1):51–56

Henning AL, Jiang MX, Yalcin HC, Butcher JT (2011) Quantitative three-dimensional imaging of live avian embryonic morphogenesis via micro-computed tomography. Dev Dyn 240(8):1949–1957

Hickerson A, Rinderknecht D, Gharib M (2005) Experimental study of the behavior of a valveless impedance pump. Exp Fluids 39(4):787–787, 0723-4864

Hickerson AI, Gharib M (2006) On the resonance of a pliant tube as a mechanism for valveless pumping. J Fluid Mech 555-1:141–148

Hierck BP, Van der Heiden K, Poelma C, Westerweel J, Poelmann RE (2008) Fluid shear stress and inner curvature remodeling of the embryonic heart. Choosing the right lane! Sci World J 8:212–222

Hochel J, Akiyama R, Masuko T, Pearson JT, Nichelmann M, Tazawa H (1998) Development of heart rate irregularities in chick embryos. Am J Physiol 275(2 Pt 2):H527–H533

Hogers B, DeRuiter MC, Gittenberger-de Groot AC, Poelmann RE (1997) Unilateral vitelline vein ligation alters intracardiac blood flow patterns and morphogenesis in the chick embryo. Circ Res 80(4):473–481

Hogers B, DeRuiter MC, Gittenberger-de Groot AC, Poelmann RE (1999) Extraembryonic venous obstructions lead to cardiovascular malformations and can be embryolethal. Cardiovasc Res 41(1):87–99

Hou PC, Burggren WW (1995) Cardiac output and peripheral resistance during larval development in the anuran amphibian xenopus laevis. Am J Physiol 269(5 Pt 2):R1126–R1132

Hove J (2006) Quantifying cardiovascular flow dynamics during early development. Pediatr Res 60(1):6–13

Hove JR, Köster RW, Forouhar AS, Acevedo-Bolton G, Fraser SE, Gharib M (2003) Intracardiac fluid forces are an essential epigenetic factor for embryonic cardiogenesis. Nature 421(6919):172–177

Hu N, Clark EB (1989) Hemodynamics of the stage 12 to stage 29 chick embryo. Circ Res 65(6):1665–1670

Hu N, Keller BB (1995) Relationship of simultaneous atrial and ventricular pressures in stage 16–27 chick embryos. Am J Physiol 269(4 Pt 2):H1359–H1362

Hu N, Connuck DM, Keller BB, Clark EB (1991) Diastolic filling characteristics in the stage 12 to 27 chick embryo ventricle. Pediatr Res 29(4 Pt 1):334–337

Hu N, Sedmera D, Yost HJ, Clark EB (2000) Structure and function of the developing zebrafish heart. Anat Rec 260(2):148–157

Icardo J, Fernandez-Teran A (1987) Morphologic study of ventricular trabeculation in the embryonic chick heart. Acta Anat 130(3):264–274

Ishiwata T, Nakazawa M, Pu WT, Tevosian SG, Izumo S (2003) Developmental changes in ventricular diastolic function correlate with changes in ventricular myoarchitecture in normal mouse embryos. Circ Res 93(9):857–865

Itasaki N, Nakamura H, Sumida H, Yasuda M (1991) Actin bundles on the right side in the caudal part of the heart tube play a role in dextro-looping in the embryonic chick heart. Anat Embryol (Berl) 183(1):29–39

Jacob E, Drexel M, Schwerte T, Pelster B (2002) Influence of hypoxia and of hypoxemia on the development of cardiac activity in zebrafish larvae. Am J Physiol-Reg I 283(4):R911–R917

Jenkins M, Adler D, Gargesha M, Huber R, Rothenberg F, Belding J, Watanabe M, Wilson D, Fujimoto J, Rollins A (2007) Ultrahigh-speed optical coherence tomography imaging and visualization of the embryonic avian heart using a buffered fourier domain mode locked laser. Opt Express 15:6251–6267

Jenkins M, Chughtai O, Basavanhally A, Watanabe M, Rollins A (2007b) In vivo imaging of the embryonic heart using gated optical coherence tomography. J Biomed Opt 12:030505

Jenkins M, Watanabe M, Rollins A (2012) Longitudinal imaging of heart development with optical coherence tomography. IEEE J Sel Top Quant Electron 18(3):1166–1175

Jones E, Baron M, Fraser S, Dickinson M (2004) Measuring hemodynamic changes during mammalian development. Am J Physiol Heart C 287(4):H1561–H1569

Jung E (2007) A mathematical model of valveless pumping: a lumped model with time-dependent compliance, resistance, and inertia. Bull Math Biol 69(7):2181–2198

Jung E, Peskin CS (2001) Two-dimensional simulations of valveless pumping using the immersed boundary method. SIAM J Sci Comput 23(1):19–45

Kamino K, Hirota A, Fujii S (1981) Localization of pacemaking activity in early embryonic heart monitored using voltage-sensitive dye. Nature 290(5807):595–597

Keller BB (1998) Embryonic cardiovascular function, coupling and maturation: a species view. In: Burggren W, Keller B (eds) Development of cardiovascular systems. University Press, Cambridge

Keller BB, Hu N, Clark EB (1990) Correlation of ventricular area, perimeter, and conotruncal diameter with ventricular mass and function in the chick embryo from stages 12 to 24. Circ Res 66(1):109–114

Keller BB, Hu N, Serrino PJ, Clark EB (1991) Ventricular pressure-area loop characteristics in the stage 16 to 24 chick embryo. Circ Res 68(1):226–231

Keller BB, Tinney JP, Hu N (1994) Embryonic ventricular diastolic and systolic pressure–volume relations. Cardiol Young 4(01):19–27

Keller BB, MacLennan MJ, Tinney JP, Yoshigi M (1996) In vivo assessment of embryonic cardiovascular dimensions and function in day-10.5 to -14.5 mouse embryos. Circ Res 79(2):247–255

Kenner T, Moser M, Tanev I, Ono K (2000) The liebau-effect or on the optimal use of energy for the circulation of blood. Scripta Medica 73(1):9–14

Kilner PJ (2005) Valveless pump models that laid a false but fortuitous trail on the way towards the total cavopulmonary connection. Cardiol Young 15(SupplementS3):74–79

Kim JS, Min J, Recknagel AK, Riccio M, Butcher JT (2011) Quantitative three-dimensional analysis of embryonic chick morphogenesis via microcomputed tomography. Anat Rec (Hoboken) 294(1):1–10

Kirchhoff S, Kim JS, Hagendorff A, Thönnissen E, Krüger O, Lamers WH, Willecke K (2000) Abnormal cardiac conduction and morphogenesis in connexin40 and connexin43 double-deficient mice. Circ Res 87(5):399–405

Kowalski W, Teslovich N, Dur O, Keller B, Pekkan K (2012) Computational hemodynamic optimization predicts dominant aortic arch selection is driven by embryonic outflow tract orientation in the chick embryo. Biomech Model Mechanobiol [Epub ahead of print]

Kunz P, Crelier GR, Schwizer W, Borovicka J, Kreiss C, Fried M, Boesiger P (1998) Gastric emptying and motility: assessment with mr imaging–preliminary observations. Radiology 207(1):33–40

Lakkis MM, Epstein JA (1998) Neurofibromin modulation of ras activity is required for normal endocardial-mesenchymal transformation in the developing heart. Development 125(22):4359–4367

Lamers W, Moorman A (2002) Cardiac septation: a late contribution of the embryonic primary myocardium to heart morphogenesis. Circ Res 91:93–103

Latacha KS, Rémond MC, Ramasubramanian A, Chen AY, Elson EL, Taber LA (2005) Role of actin polymerization in bending of the early heart tube. Dev Dyn 233(4):1272–1286

Lee K, Simon H, Chen H, Bates B, Hung M, Hauser C (1995) Requirement for neuregulin receptor erbb2 in neural and cardiac development. Nature 378(6555):394–398

Liebau G (1954) Uber ein ventilloses pumpprinzip. Z Kreislaufforsch 41(14):327–328

Liebau G (1957) Significance of forces of inertia in the dynamics of blood circulation. Z Kreislaufforsch 46(11–12):428–438

Lin IE, Taber LA (1995) A model for stress-induced growth in the developing heart. J Biomech Eng 117:343–349

Lincoln J, Alfieri CM, Yutzey KE (2004) Development of heart valve leaflets and supporting apparatus in chicken and mouse embryos. Dev Dyn 230(2):239–250

Ling P, Taber L, Humphrey J (2002) Approach to quantify the mechanical behavior of the intact embryonic chick heart. Ann Biomed Eng 30:636–645

Liu A, Nickerson A, Troyer A, Yin X, Cary R, Thornburg K, Wang R, Rugonyi S (2011) Quantifying blood flow and wall shear stresses in the outflow tract of chick embryonic hearts. Comput Struct 89(11–12):855–867

Loots E, Hillen B, Veldman AEP (2003) The role of hemodynamics in the development of the outflow tract of the heart. J Eng Math 45(1):91–104, 0022-0833

Loumes L, Avrahami I, Gharib M (2008) Resonant pumping in a multilayer impedance pump. Phys Fluids 20(2):023–103

Lucitti JL, Tobita K, Keller BB (2005) Arterial hemodynamics and mechanical properties after circulatory intervention in the chick embryo. J Exp Biol 208(Pt 10):1877–1885

Ma L, Lu MF, Schwartz RJ, Martin JF (2005) Bmp2 is essential for cardiac cushion epithelial-mesenchymal transition and myocardial patterning. Development 132(24):5601–5611

Ma Z, Liu A, Yin X, Troyer A, Wang R, Rugonyi S (2010) Absolute flow velocity measurement in hh18 chicken embryo outflow tract based on 4d reconstruction using spectral domain optical coherence tomography. Biomed Opt Express 1:798–811

Männer J (2000) Cardiac looping in the chick embryo: a morphological review with special reference to terminological and biomechanical aspects of the looping process. Anat Rec 259(3):248–262

Männer J (2004) On rotation, torsion, lateralization, and handedness of the embryonic heart loop: new insights from a simulation model for the heart loop of chick embryos. Anat Rec A Discov Mol Cell Evol Biol 278(1):481–492

Manner J, Thrane L, Norozi K, Yelbuz T (2008) High-resolution in vivo imaging of the cross-sectional deformations of contracting embryonic heart loops using optical coherence tomography. Dev Dyn 237(4):953–961

Manner J, Thrane L, Norozi K, Yelbuz T (2009) In vivo imaging of the cyclic changes in cross-sectional shape of the ventricular segment of pulsating embryonic chick hearts at stages 14 to 17: a contribution to the understanding of the ontogenesis of cardiac pumping function. Dev Dyn 238(12):3273–3278

Manner J, Wessel A, Yelbuz TM (2010) How does the tubular embryonic heart work? Looking for the physical mechanism generating unidirectional blood flow in the valveless embryonic heart tube. Dev Dyn 239(4):1035–1046

Maron BJ, Hutchins GM (1974) The development of the semilunar valves in the human heart. Am J Pathol 74(2):331–344

Martinsen BJ (2005) Reference guide to the stages of chick heart embryology. Dev Dyn 233(4):1217–1237

Mercola M, Levin M (2001) Left-right asymmetry determination in vertebrates. Annu Rev Cell Dev Biol 17:779–805

Meyer D, Birchmeier C (1995) Multiple essential functions of neuregulin in development. Nature 378(6555):386–390

Miller CE, Wong CL, Sedmera D (2003) Pressure overload alters stress-strain properties of the developing chick heart. Am J Physiol Heart C 285(5):H1849–H1856

Miura GI, Yelon D (2011) A guide to analysis of cardiac phenotypes in the zebrafish embryo. Methods Cell Biol 101:161–180

Moser M, Huang JW, Schwarz GS, Kenner T, Noordergraaf A (1998) Impedance defined flow generalisation of william harvey's concept of the circulation—370 years later. Int J Cardiovasc Med Sci 1:205–211

Nomura-Kitabayashi A, Phoon CKL, Kishigami S, Rosenthal J, Yamauchi Y, Abe K, Yamamura Ki, Samtani R, Lo CW, Mishina Y (2009) Outflow tract cushions perform a critical valve-like function in the early embryonic heart requiring bmpria-mediated signaling in cardiac neural crest. Am J Physiol Heart C 297(5):H1617–H1628

Ong LL, Kim N, Mima T, Cohen-Gould L, Mikawa T (1998) Trabecular myocytes of the embryonic heart require n-cadherin for migratory unit identity. Dev Biol 193(1):1–9

Oostra RJ, Steding G, Virágh S (2007) Steding's and Virágh's scanning electron microscopy atlas of the developing human heart. Springer, New York

O'Rahilly R, Muller F (1987) Developmental stages in human embryos. Carnegie Institution Washington Publication, Washington, DC 673

O'Rahilly R, Muller F (2010) Developmental stages in human embryos: revised and new measurements. Cells Tissues Organs 192(2):73–84

Ottesen JT (2003) Valveless pumping in a fluid-filled closed elastic tube-system: one-dimensional theory with experimental validation. J Math Biol 46(4):309–332

Paff GH (1940) A micro-method for digitalis assay. J Pharmacol Exp Ther 69(4):311–315

Paff GH, Johnson JR (1938) The behavior of the embryonic heart in solutions of ouabain. Am J Physiol 122(3):753–758

Paff GH, Boucek RJ, Klopfenstein HS (1964) Experimental heart-block in the chick embryo. Anat Rec 149:217–223

Parpart ER, Glaser O (1929) Temperature and heart rate in chick embryos. J Exp Biol 7:143–153

Pelster B, Burggren WW (1996) Disruption of hemoglobin oxygen transport does not impact oxygen-dependent physiological processes in developing embryos of zebra fish (danio rerio). Circ Res 79(2):358–362

Phelan CM, Hughes SF, Benson JDW (1995) Heart rate-dependent characteristics of diastolic ventricular filling in the developing chick embryo. Pediatr Res 37(3):289–293

Phoon C, Turnbull D (2003) Ultrasound biomicroscopy-doppler in mouse cardiovascular development. Physiol Genomics 14(1):3–15

Phoon C, Ji R, Aristizabal O, Worrad D, Zhou B, Baldwin H, Turnbull D (2004) Embryonic heart failure in nfatc1-/- mice: novel mechanistic insights from in utero ultrasound biomicroscopy. Circ Res 95(1):92–99

Poelmann R, Gittenberger-de Groot A, Hierck B (2008) The development of the heart and microcirculation: role of shear stress. Med Biol Eng Comput 46:479–484

Rauhut-Klaban M, Bruska M, Woźniak W (2008) Early trabeculation and closure of the interventricular foramen in staged human embryos. Folia Morphol (Warsz) 67(1):13–18

Reckova M, Rosengarten C, de Almeida A, Stanley CP, Wessels A, Gourdie RG, Thompson RP, Sedmera D (2003) Hemodynamics is a key epigenetic factor in development of the cardiac conduction system. Circ Res 93(1):77–85

Rodbard S (1956) Vascular modifications induced by flow. Am Heart J 51(6):926–942

Rodriguez EK, Hoger A, McCulloch AD (1994) Stress-dependent finite growth in soft elastic tissues. J Biomech 27(4):455–467

Rugonyi S, Shaut C, Liu A, Thornburg K, Wang RK (2008) Changes in wall motion and blood flow in the outflow tract of chick embryonic hearts observed with optical coherence tomography after outflow tract banding and vitelline-vein ligation. Phys Med Biol 53(18):5077–5091

Rychter Z (1978) Analysis of relations between aortic arches and aorticopulmonary septation. Birth Defects Orig Artic Ser 14(7):443–448

Rychter Z, Rychterova V (1981) Angio- and myoarchitecture of the heart wall under normal and experimentally changed morphogenesis. Raven Press, New York 431–452

Rychter Z, Rychterova V, Lemez L (1979) Formation of the heart loop and proliferation structure of its wall as a base for ventricular septation. Herz 4:86–90

Rychterova V (1971) Principle of growth in thickness of the heart ventricular wall in the chick embryo. Folia Morphol (Praha) 19:262–272

Santhanakrishnan A, Miller L (2011) Fluid dynamics of heart development. Cell Biochem Biophys 61(1):1–22

Savagner P (2001) Leaving the neighborhood: molecular mechanisms involved during epithelial-mesenchymal transition. Bioessays 23(10):912–923

Sedmera D, Pexieder T, Hu N, Clark EB (1997) Developmental changes in the myocardial architecture of the chick. Anat Rec 248(3):421–432

Sedmera D, Pexieder T, Rychterova V, Hu N, Clark EB (1999) Remodeling of chick embryonic ventricular myoarchitecture under experimentally changed loading conditions. Anat Rec 254(2):238–252

Sedmera D, Hu N, Weiss KM, Keller BB, Denslow S, Thompson RP (2002) Cellular changes in experimental left heart hypoplasia. Anat Rec 267(2):137–145

Smith T, Bader D (2007) Signals from both sides: control of cardiac development by the endocardium and epicardium. Semin Cell Dev Biol 18(1):84–89

Srivastava D (2006) Genetic regulation of cardiogenesis and congenital heart disease. Annu Rev Pathol 1:199–213

Stalsberg H (1970) Development and ultrastructure of the embryonic heart. ii. mechanism of dextral looping of the embryonic heart. Am J Cardiol 25(3):265–271

Stekelenburg-de Vos S, Ursem NTC, Hop WCJ, Wladimiroff JW, Gittenberger-de Groot AC, Poelmann RE (2003) Acutely altered hemodynamics following venous obstruction in the early chick embryo. J Exp Biol 206(Pt 6):1051–1057

Stekelenburg-de Vos S, Steendijk P, Ursem NT, Wladimiroff JW, Delfos R, Poelmann RE (2005) Systolic and diastolic ventricular function assessed by pressure–volume loops in the stage 21 venous clipped chick embryo. Pediatr Res 57(1):16–21

Taber LA (1991) On a nonlinear theory for muscle shells: part ii–application to the beating left ventricle. J Biomech Eng 113(1):63–71

Taber LA (1998) Mechanical aspects of cardiac development. Prog Biophys Mol Biol 69(2–3):237–255

Taber LA, Humphrey J (2001) Stress-modulated growth, residual stress, and vascular heterogeneity. J Biomech Eng 123:528–535

Taber LA, Lin IE, Clark EB (1995) Mechanics of cardiac looping. Dev Dyn 203(1):42–50

Taber LA, Zhang J, Perucchio R (2007) Computational model for the transition from peristaltic to pulsatile flow in the embryonic heart tube. J Biomech Eng 129(3):441–449

Tobita K, Keller BB (2000) Right and left ventricular wall deformation patterns in normal and left heart hypoplasia chick embryos. Am J Physiol Heart C 279(3):H959–H969

Tobita K, Schroder EA, Tinney JP, Garrison JB, Keller BB (2002) Regional passive ventricular stress-strain relations during development of altered loads in chick embryo. Am J Physiol Heart C 282(6):H2386–H2396

Tomlins P, Wang R (2005) Theory, development and applications of optical coherence tomography. J Phys D Appl Phys 38:2519–2535

Ursem NTC, Stekelenburg-de Vos S, Wladimiroff JW, Poelmann RE, Gittenberger-de Groot AC, Hu N, Clark EB (2004) Ventricular diastolic filling characteristics in stage-24 chick embryos after extraembryonic venous obstruction. J Exp Biol 207(Pt 9):1487–1490

Usha S, Rao AR (1995) Peristaltic transport of a biofluid in a pipe of elliptic cross section. J Biomech 28(1):45–52

Van den Berg G, Moorman A (2009) Concepts of cardiac development in retrospect. Pediatr Cardiol 30:580–587

Van der Heiden K, Groenendijk B, Hierck B, Hogers B, Koerten H, Mommaas A, Gittenberger-de Groot A, Poelmann R (2006) Monocilia on chicken embryonic endocardium in low shear stress areas. Dev Dyn 235:19–28

Vennemann P, Kiger KT, Lindken R, Groenendijk BC, Stekelenburg-de Vos S, ten Hagen TL, Ursem NT, Poelmann RE, Westerweel J, Hierck BP (2006) In vivo micro particle image velocimetry measurements of blood-plasma in the embryonic avian heart. J Biomech 39(7):1191–1200

Vermot J, Forouhar A, Liebling M, Wu D, Plummer D, Gharib M, Fraser S (2009) Reversing blood flows act through klf2a to ensure normal valvulogenesis in the developing heart. PLoS Biol 7(11):2511–2524

Voronov DA, Taber LA (2002) Cardiac looping in experimental conditions: effects of extraembryonic forces. Dev Dyn 224(4):413–421

Voronov DA, Alford PW, Xu G, Taber LA (2004) The role of mechanical forces in dextral rotation during cardiac looping in the chick embryo. Dev Biol 272(2):339–350

Wagman AJ, Hu N, Clark EB (1990) Effect of changes in circulating blood volume on cardiac output and arterial and ventricular blood pressure in the stage 18, 24, and 29 chick embryo. Circ Res 67(1):187–192

Wagner M, Siddiqui MAQ (2007) Signal transduction in early heart development (ii): ventricular chamber specification, trabeculation, and heart valve formation. Exp Biol Med (Maywood) 232(7):866–880

Wang Y, Dur O, Patrick MJ, Tinney JP, Tobita K, Keller BB, Pekkan K (2009) Aortic arch morphogenesis and flow modeling in the chick embryo. Ann Biomed Eng 37(6):1069–1081

Warkman AS, Krieg PA (2007) Xenopus as a model system for vertebrate heart development. Semin Cell Dev Biol 18(1):46–53

Yalcin HC, Shekhar A, Nishimura N, Rane AA, Schaffer CB, Butcher JT (2010) Two-photon microscopy-guided femtosecond-laser photoablation of avian cardiogenesis: noninvasive creation of localized heart defects. Am J Physiol Heart C 299(5):H1728–H1735

Yalcin HC, Shekhar A, McQuinn TC, Butcher JT (2011) Hemodynamic patterning of the avian atrioventricular valve. Dev Dyn 240(1):23–35

Yang M, Taber LA, Clark EB (1994) A nonlinear poroelastic model for the trabecular embryonic heart. J Biomech Eng 116(2):213–223

Yoshigi M, Keller B (1997) Characterization of embryonic aortic impedance with lumped parameter models. Am J Physiol Heart C 42(1):H19–H27

Zhou YQ, Foster FS, Qu DW, Zhang M, Harasiewicz KA, Adamson SL (2002) Applications for multifrequency ultrasound biomicroscopy in mice from implantation to adulthood. Physiol Genomics 10(2):113–126